



LAWRENCE
LIVERMORE
NATIONAL
LABORATORY

Model-Based Estimation of Forest Canopy Height in Red and Austrian Pine Stands Using Shuttle Radar Topography Mission and Ancillary Data: a Proof-of-Concept Study

Charles G. Brown Jr., Kamal Sarabandi, Leland E.
Pierce

April 10, 2007

IEEE TRANSACTIONS ON GEOSCIENCE AND REMOTE
SENSING

Disclaimer

This document was prepared as an account of work sponsored by an agency of the United States government. Neither the United States government nor Lawrence Livermore National Security, LLC, nor any of their employees makes any warranty, expressed or implied, or assumes any legal liability or responsibility for the accuracy, completeness, or usefulness of any information, apparatus, product, or process disclosed, or represents that its use would not infringe privately owned rights. Reference herein to any specific commercial product, process, or service by trade name, trademark, manufacturer, or otherwise does not necessarily constitute or imply its endorsement, recommendation, or favoring by the United States government or Lawrence Livermore National Security, LLC. The views and opinions of authors expressed herein do not necessarily state or reflect those of the United States government or Lawrence Livermore National Security, LLC, and shall not be used for advertising or product endorsement purposes.

Model-Based Estimation of Forest Canopy Height in Red and Austrian Pine Stands Using Shuttle Radar Topography Mission and Ancillary Data: a Proof-of-Concept Study

Charles G. Brown Jr., Kamal Sarabandi, and Leland E. Pierce

August 4, 2009

Abstract

In this paper accurate tree stand height retrieval is demonstrated using C-band Shuttle Radar Topography Mission (SRTM) height and ancillary data. The tree height retrieval algorithm is based on modeling uniform tree stands with a single layer of randomly-oriented vegetation particles. For such scattering media, the scattering phase center (SPC) height, as measured by SRTM, is a function of tree height, incidence angle, and the extinction coefficient of the medium. The extinction coefficient for uniform tree stands is calculated as a function of tree height and density using allometric equations and a fractal tree model. The accuracy of the proposed algorithm is demonstrated using SRTM and TOPSAR data for 15 red pine and Austrian pine stands. (TOPSAR is an airborne interferometric synthetic aperture radar.) The algorithm yields rms errors of 2.5 to 3.6m, which is substantial

The first author is currently with Lawrence Livermore National Laboratory, Livermore, CA 94550. The other authors are with the Radiation Laboratory, Department of Electrical and Computer Engineering, University of Michigan, Ann Arbor, MI 48109. Most of the work for this article was performed at the University of Michigan under NASA Grant NAG5-8930, or otherwise outside of Lawrence Livermore National Laboratory, and published under the auspices of the U.S. Department of Energy by Lawrence Livermore National Laboratory under Contract DE-AC52-07NA27344. UCRL-JRNL-229808

improvement over the 6.8 to 8.3m rms errors from the raw SRTM minus National Elevation Dataset (NED) heights.

Index Terms

Remote sensing, Synthetic aperture radar, Interferometry

I. INTRODUCTION

One set of forest structural components that is not well measured by the current Earth Observing System is forest vertical structure parameters, such as tree height. This paper presents an algorithm, based on an electromagnetic scattering model, to estimate tree stand height using data from an interferometric synthetic aperture radar (INSAR) mission, the Shuttle Radar Topography Mission (SRTM) [1], in conjunction with ancillary data.

Interferometric synthetic aperture radar (INSAR) is ideal for retrieval of forest structure, since it has been shown to be particularly sensitive to forest vertical structure parameters, such as extinction and height [2], [3], [4]. Multiple-baseline INSAR and polarimetry are used in [5] to estimate an additional parameter, the ground-to-volume scattering ratio. Further, trunk diameter, tree height, tree density, branching angle, soil moisture, and wood moisture are retrieved from INSAR data from multiple incidence angles in [6]. Fully polarimetric INSAR (POLINSAR) [3], [7], [8] is sensitive to the distribution and orientation of scatterers, further increasing the set of canopy parameters that can be estimated [9]. Encouraging results have been obtained from POLINSAR [8], [10]. A newer POLINSAR approach is in [11]. An additional estimation scenario [5] employs multi-altitude, multi-frequency polarimetric SAR and INSAR data to determine vertical extinction profiles in addition to a set of usual parameters such as height, ground to volume scattering ratio, etc. Some stem volume retrieval methods requiring training, which use ERS-1/2 and JERS multitemporal interferometry, are in [12], [13]. The data sets upon which these studies are based are multitemporal, such as from ERS-1/2 and JERS, or are highly localized, like those produced by airborne INSAR or special spaceborne, multitemporal INSAR missions that were not global, unlike

SRTM. In the past several years, progress has been made in retrieving forest structural parameters using the SRTM data set [14], [15], [16], [17]. This paper reports the novel approach in [14], [15], which retrieves tree stand height from SRTM and ancillary data employing an algorithm based on an electromagnetic scattering model, not using an empirical regression model derived from ground truth measurements, as in [16].

II. BACKGROUND

The basic measurement provided by SRTM is an INSAR height, with respect to a reference surface (see Section III). When trees are present, the INSAR height above the underlying ground height tends to be less than the tree heights, since SRTM penetrates the tree canopy to a certain extent. In this paper we define the *SRTM scattering phase center (SPC) height* to be the SRTM INSAR height minus the underlying ground height, in order to distinguish it from the SRTM INSAR height. Tree height, density, and other forest vertical structure parameters (see Section I), as well as INSAR geometry parameters like incidence angle, affect the SRTM SPC height. Ideally, we would like to have an inverse model like the one pictured in Fig. 1, where the SRTM SPC height \bar{h}_{SPC} is taken as the input, and the model outputs an estimate of the average height \hat{h}_v of a tree stand. However, due to the complex nature of scattering mechanisms in such an environment, it seems extremely difficult, if not impossible, to create such a direct inverse model.

The basic strategy used in the studies listed above to determine forest vertical structure parameters, with the exceptions of [16], [17], is to develop theory-based, forward-scattering models describing SAR, INSAR, and POLINSAR observables as a function of canopy parameters. The models are usually simplified to include only the most influential parameters of interest. The forward models are then inverted to yield forest vertical structure parameters as a function of SAR, INSAR, and POLINSAR observables, often using an iterative scheme similar to Fig. 2, which is specialized for SRTM SPC height. The literature concerning SAR/INSAR forest parameter retrieval indicates that a successful algorithm would require a larger number of independent radar observables than we have from SRTM INSAR heights alone [2], [3], [4], [5], [6], [7],

[9], [18], [19], [8]. However, use of additional *a priori* information (c.f. [8]) such as underlying ground topography from other sources (c.f. [20], [21], [22], [16]), extinction coefficient measurements [2], etc. can reduce the number of observables necessary. In our case we use ground topography maps to convert SRTM INSAR heights to SRTM SPC heights. Then we employ species structure and tree density and moisture estimates to allow us to retrieve tree stand height from the SRTM SPC heights.

We proceed by first describing how to obtain SRTM SPC height from the SRTM INSAR height data. Then we discuss a simple forward model that relates the tree stand height h_v , among other parameters, to SRTM SPC height \bar{h}_{SPC} . Finally, we present a method for inverting the forward model and describe our test results.

III. SRTM SCATTERING PHASE CENTER HEIGHT

The INSAR heights given in the SRTM data are elevations with respect to the World Geodetic System 1984 (WGS84) geoid. However, the inverse model depicted in Fig. 2 requires the SRTM SPC height, which is the SRTM height minus the height of the ground, as defined in Section II. We obtain an estimate of this quantity by subtracting the National Elevation Dataset (NED) heights [23], [24] from the SRTM Ground Data Processing System (GDPS) heights. We use the Principal Investigator (PI) data for incidence angle and polarization information. References [20], [21], [22], [16] use a similar method to obtain estimates of SPC height from airborne INSAR and spaceborne SRTM data. The SRTM GDPS data for this tree height retrieval were obtained from [25]. We obtained NED data from the EROS Data Center at [26]. The SRTM GDPS data also are available there.

The SRTM GDPS and the NED work particularly well together, since both use nearly identical datums. The horizontal datum of the SRTM GDPS is the WGS84. Its vertical datum is the WGS84 geoid. The NED has as its horizontal and vertical datums the North American Datum 1983 (NAD83) and the North American Vertical Datum (NAVD88), respectively. For meter-level accuracy, WGS84 and NAD83 for the conterminous United States are effectively identical [27]. Also, heights in the WGS84 and NAVD88 vertical datums are within a meter or so. If greater accuracy is needed, there are means of converting

between the various horizontal and vertical datums [28], [29], [30]. However, since the errors in the SRTM GDPS heights are on the order of a few meters [15], [31], it is generally not necessary to do so.

Other errors in the SRTM minus NED heights are due to systematic and random noise in the SRTM data (c.f. [15], [31], [16]). In order to assess the systematic topographical noise, we examine the SRTM minus NED heights, obtained from [32], for a large cultivated area (nearly 200 30m by 30m SRTM pixels) near our test site, where the difference between the SRTM and NED heights should be nearly zero. The cultivated area is identified using the National Land Cover Data Set (NLCD) 2001 [32]. The mean difference over that area is 0.2m, indicating acceptably small systematic error for our desired meter-order accuracy. The standard deviation of the difference over the cultivated area is 1.7m. However, since we average several to many pixels in application of our method, the random noise is reduced [16]. The standard deviation range of the random noise range for our size stands (see Section VI) is less than approximately 0.8m to 1.6m, assuming pixels are averaged over uniform tree stands.

IV. FORWARD MODEL

There are several electromagnetics-based INSAR forward models available in the literature to relate tree stand height h_v to SPC height, such as in [2], [3], [4], [18], [19], [33], [34], [35], which is by no means an exhaustive list. Since we wish to estimate tree stand height based on SRTM SPC height alone (i.e. no other SAR/INSAR observables), we must choose as simple of a model as possible. The single-layer, randomly-oriented vegetation scattering model with no ground interaction [2], [19], [34] is perhaps the best model for this task. The simplicity criterion is not the only support for using such a model. Even though the tree stands we test our model on do not constitute an infinite single layer [36], the results (Section VI) indicate that the effect of the ground interaction at C-band is small enough compared to that of the direct backscatter so that we can achieve accuracy on the order of a few meters. Such accuracy is at least sufficient for rough height binning. Future work could include extension to a forward model with ground and ground-bounce returns, if further accuracy is necessary.

A. Single-Layer, Randomly-Oriented Vegetation Scattering Model

The SRTM INSAR height data for the end user is an average of the INSAR heights of the individual SRTM overpasses. Thus, the SRTM SPC height \bar{h}_{SPC} computed from the SRTM INSAR height data can be modeled as

$$\bar{h}_{SPC} = \frac{1}{N} \sum_{i=1}^N h_{SPC_i},$$

where h_{SPC_i} denotes the SRTM SPC height derived from the i^{th} overpass. We can write h_{SPC_i} as the output of the SPC height model \mathcal{M}_i as a function of the parameters most pertinent to the simple forward model we use:

$$h_{SPC_i} = \mathcal{M}_i(h_v; k_0, H, B, \alpha, \theta_i, n, M_w, M_f, p_i \dots),$$

with h_v being the average height of the tree stand (what we want to estimate). See Fig. 3. k_0 is the SRTM free-space wavenumber at its center frequency; H is the height of SRTM from the surface of the earth; B is the baseline length, and α is the baseline angle; θ_i is the incidence angle of the i^{th} overpass; n is the tree density; M_w and M_f are the moisture contents of the wood and the foliage, respectively; and p_i is the polarization (VV or HH) of the i^{th} overpass. We explicitly state the model, of which the phase term is from [2], [3], [34], as follows:

$$\begin{aligned} \mathcal{M}_i(h_v; k_0, H, \dots) &= \frac{r_i \sin \theta_i}{k_0 B \cos(\theta_i - \alpha)} \text{Arg} \left[\int_0^{h_v} e^{j\alpha_{z_i} z'} e^{\gamma_i z'} dz' \right] \\ &= \frac{r_i \sin \theta_i}{k_0 B \cos(\theta_i - \alpha)} \tan^{-1} \left[\frac{\gamma_i \sin(\alpha_{z_i} h_v) - \alpha_{z_i} \cos(\alpha_{z_i} h_v) + \alpha_{z_i} e^{-\gamma_i h_v}}{\gamma_i \cos(\alpha_{z_i} h_v) - \gamma_i e^{-\gamma_i h_v} + \alpha_{z_i} \sin(\alpha_{z_i} h_v)} \right], \end{aligned}$$

with

$$\begin{aligned} r_i &= \frac{H}{\cos \theta_i} \\ \alpha_{z_i} &= \frac{k_0 B \cos(\theta_i - \alpha)}{r_i \sin \theta_i} \end{aligned}$$

$$\gamma_i = \frac{2\kappa_{e_i}}{\cos \theta_i}.$$

Note that the parameters beyond the semicolon in \mathcal{M}_i are now implied. “Arg” denotes the radian phase on the interval $(-\pi, \pi]$, and $j = \sqrt{-1}$. The extinction coefficient κ_{e_i} (Nepers/m) is a function of $h_v, n, \theta_i, M_w, M_f, p_i$, and other parameters:

$$\kappa_{e_i} = \mathcal{P}_i(h_v, n; \theta_i, M_w, M_f, p_i, \dots).$$

Similar to the situation in [2], the SRTM SPC height alone does not provide enough measurements to estimate h_v and κ_{e_i} . Instead of deriving the extinction coefficient values from measurements, as in [2], we relate κ_{e_i} to h_v and other variables, which possibly are easier to estimate than the extinction coefficient itself, using allometric relations and a fractal model. We will detail the development of the extinction coefficient model \mathcal{P}_i in the subsections to follow. First, we present the fractal tree model used to compute \mathcal{P}_i . Then, we calculate the allometric equations necessary to specify the fractal models. Finally, we describe the process of computing \mathcal{P}_i using the fractal tree models, and we present the resulting \mathcal{P}_i model.

B. Red Pine Fractal Tree Models

The fractal trees used in this study are the red pine fractal models pioneered in [6], [18], [33], since that is the dominant species in our test stands. The red pine model also is used to represent a structurally similar species, Austrian pine. The fractal modeling method is general-purpose and can be used for both coniferous and broadleaf trees. However, in this proof-of-concept work, only two coniferous species are considered.

We modified the fractal tree generation code used in [6], [18], [33] and added a graphical user interface (GUI) to more easily create tree models of different species, or of different heights, crown sizes, etc. within the same species. As in [6], [18], [33], the user designs a “DNA” file that encodes species-specific information about the structure of the tree using the tree designer GUI. In order to produce a specific realization of a red pine, the user provides tree height, diameter at breast height (dbh), crown depth, and

crown radius. The tree-generating code then produces a realization of a red pine with the specified height, dbh, crown depth, and crown radius. Each tree thus produced is identical only in a statistical sense, even if the same height, dbh, crown depth, and crown radius are specified, since the code introduces a certain amount of randomness to the tree structure according to the DNA file. Each tree is composed of thousands of lossy cylinders of varying lengths and radii that form the trunk, branches, needles, etc.

C. Red Pine Allometric Equations

As stated in the previous subsection, the fractal model needs tree height, dbh, crown depth, and crown radius in order to produce a specific realization of a red pine. Ideally, we would like to have the fractal model specified by only tree height, since that is the parameter we are estimating. However, the best we can do is to specify the fractal model as a function of tree height and density through allometric equations that relate dbh, crown depth, and crown radius to tree height and density. The red pine allometric equations are developed using ground truth data from the Raco, Michigan SIR-C/X-SAR Supersite [37]. A total of 17 red pine stands are used in the allometric equation calculations relating height (m), dbh (cm), and crown depth (m). Figures 4 and 5 depict the red pine data and the resulting polynomial fits to the data. The allometric equations are

$$\text{dbh} = 1.4939h_v + 2.2267, \text{ and}$$

$$\text{crown depth} = -0.02559h_v^2 + 1.0193h_v - 0.093364.$$

Another parameter required by the fractal model is crown radius. We have no data from Raco, Michigan for crown radius, but it is reasonable to assume we can approximate the actual values by relating crown radius to tree density n in trees per hectare (ha) by invoking simple physical packing limitations. We assume that crown radius is half of the average spacing between the trees, where the average spacing in meters is determined from the tree density n : average spacing = $\sqrt{10000/n}$, where 10000 square meters per hectare is the conversion factor between area in hectares and area in square meters. However, crown radius does not continue to grow without bound with decreasing n , so we arbitrarily fix the maximum crown

radius at 2m. Since the average tree spacing for $n=625$ trees/ha is 4m, thus yielding crown radius=2m, we can write crown radius as follows:

$$\text{crown radius} = \begin{cases} \frac{50}{\sqrt{n}} & : n \geq 625 \\ 2 & : n < 625 \end{cases},$$

where n is the number of trees per hectare. Implicit in the crown radius equation is the fact that $n \geq 0$ and that there is some unknown upper limit to n .

D. Extinction Coefficient Model

In order to develop the extinction coefficient model we vary several key parameters over wide ranges of typical values; generate red pine fractal tree models with those parameters; and compute \mathcal{P}_i according to [18], [33], employing the electromagnetic scattering code used in [6], [18], [33], with a single layer at a temperature of -2°C (28.4°F) and 5°C (41.0°F). (The temperatures are chosen to cover conditions in Section VI.) The wavelength we use is 5.8cm. First, we generate 10 realizations of red pine fractal trees for each combination of h_v and n values listed in Table I. The ranges for the h_v and n roughly bracket typical heights and densities for red pine stands. Next, for each one of those 30 combinations, we vary θ_i and $M = M_f = M_w$, where gravimetric moisture content (g water/g wet biomass) of the wood is used, with a dry bulk density of 0.392g/cm^3 [38], according to Table II, and $p_i = \text{VV}, \text{HH}$. The assumption that $M = M_f = M_w$ is supported by [39] and is invoked for simplicity. Future versions of this model could independently vary M_f and M_w . The range for the moisture content approximates the range reported in [39] for young jack pine. We linearly interpolate to give κ_{e_i} values for points not on the grid specified above. Out-of-range parameters are allowed for height only and only for heights from 0 to 5m and from 30 to 35m by linear extrapolation of \mathcal{P}_i . The simplified extinction coefficient model is expressed as

$$\kappa_{e_i} = \mathcal{P}_i(h_v; n, \theta_i, M, p_i).$$

Other parameters might have an effect on the extinction coefficient but are included implicitly in the fractal tree model (e.g., species-specific structure characteristics); set to a fixed, reasonable value; or are assumed to have second-order effect on the desired meter-level accuracy and are omitted for simplicity.

Figures 6 and 8 display \mathcal{P}_i as a function of the parameters h_v , n , θ_i , and M for VV polarization at -2°C and 5°C , respectively. The temperatures are chosen based on the average temperatures for our data set. See Section VI. Figures 7 and 9 display the same information for HH polarization at -2°C and 5°C , respectively. The format is the same for Figs. 6, 7, 8, and 9. The top row corresponds to $M = 0.3\text{g/g}$, while in the bottom row $M = 0.6\text{g/g}$. The columns, left to right, correspond to $\theta_i = 40^\circ, 50^\circ, 60^\circ$. Tree height h_v is along the x-axis of the individual subplots. Tree density n is varied within each subplot to produce the lines marked by the different symbols, where the symbols “.”, “o”, “x”, “+”, and “*” correspond to tree densities of $n = 100, 500, 900, 1300$, and 1700 trees per hectare, respectively. The extinction coefficient variation with polarization and incidence angle (in particular our range) is not nearly as strong as with tree height, density, and moisture. Note also that there is not much of a variation between -2°C and 5°C . The extinction coefficients for -2°C and 5°C are for thawed conditions. However, the -2°C extinction coefficients can be converted to approximate frozen extinction coefficients by dividing the thawed extinction coefficients by two [2].

V. INVERSION ALGORITHM

We use a golden section search over the stand height interval from 0 to 35m to invert the forward model. Refer to Fig. 10 for a flowchart of the basic inversion algorithm. The estimated tree stand height \hat{h}_v is optimized using an objective function J defined as the squared difference between the modeled SRTM SPC height \hat{h}_{SPC} and the observed SRTM SPC height \bar{h}_{SPC} : $J(\hat{h}_v; n, M) = (\hat{h}_{SPC} - \bar{h}_{SPC})^2$. In order to obtain the observed SRTM SPC height, we average the SRTM SPC heights over the tree stand. Since we use the SRTM-NED heights as an approximation for the SRTM SPC heights, as stated in Section III, we refer to the SRTM-NED heights, averaged over a tree stand, in the abbreviated form “raw SRTM-NED” height.

Here we distinguish between two different estimation scenarios, one in which tree density n and moisture M are known, and one in which we have only rough, approximate values. In both scenarios, we set n and M in J to *fixed* values. The tree density n could be obtained from ancillary sources, which could include forest growth models or other remote sensing techniques, such as individual tree crown (ITC) forest analysis using satellite images [40]. M could be set to a fixed average value selected according to location, season, and species. However, in this proof-of-concept paper in the first scenario, we fix n according to ground truth tree density and set $M=0.45\text{g/g}$, which is the average of the moisture range used to generate our extinction coefficient model. Finally, we optimize J to yield our tree stand height estimate \hat{h}_v . The second estimation scenario is more complicated, since more uncertainty is assumed in the n and M values.

In the second scenario, we assume we do not have accurate values for n and M but that we know rough, approximate values. For this proof-of-concept work we set n and M to reasonable, average values (those values are more precisely defined in Section VI) and optimize J to yield our tree stand height estimate h_v , as in the first scenario. Since there is uncertainty in n and M , we need to address the sensitivity of \hat{h}_v to errors in n and M . In the second estimation scenario we use reasonable but rough approximations for n and M and report the corresponding height estimate \hat{h}_v and a range of \hat{h}_v for the given uncertainty in n and M . For example consider Fig. 11, a contour plot of \hat{h}_v as a function of n and M for stand RP2 (see Section VI), which has a raw SRTM-NED height of 16.6m. The extinction coefficient model assumes -2°C thawed conditions, but the plot would be essentially the same for 5° . Suppose we use $n = 360$ trees/ha and $M = 0.45$ g/g for the rough, approximate values for n and M . The corresponding tree stand height estimate \hat{h}_v would be 23m. Even if n were off by $\pm 50\%$ and M were off by $\pm 33\%$, the range of the corresponding for \hat{h}_v would vary only from 21m to 26m. Figures 12 and 13 are plots like Fig. 11, except for stands AP2 and RP8 which have raw SRTM-NED heights of 2.8m and 8.9m, respectively.

In both scenarios, we must know incidence angle, polarization, platform height, free-space wavelength, and interferometric baseline parameters for each of the N SRTM overpasses. We calculate incidence

angles θ_i for each of the $i = 1, 2, 3$ SRTM overpasses that imaged the Kellogg Experimental Forest by averaging the incidence angle files of the Kellogg Principal Investigator (PI) processor data over all of our test stands. Since the area is small, we expect the incidence angle does not vary appreciably across the test stands. We obtain polarization information also from the PI processor data. The SRTM free-space wavelength was set to 5.8cm. The baseline and height parameters are taken to be $B = 60\text{m}$, $\alpha = 45^\circ$, and $H = 233\text{km}$.

VI. TEST RESULTS

We test our algorithm on 13 red pine and Austrian pine stands in the W.K. Kellogg Experimental Forest, near Battle Creek, Michigan [41]. Figure 14 is a map of the stands [42] that we investigate in this paper. The stand polygons overlay the SRTM GDPS heights minus the NED heights. Stand areas range from 3 to 45 30m by 30m SRTM pixels. The red pine stands are labeled “RP”, while the Austrian pine stands are labeled “AP”. Stand RP3 is a mixed red and white pine stand. Figure 15 is a 1996 color infrared image of the same area [43], with the darker pine stands clearly distinguished from the lighter deciduous stands. Kellogg provides an ideal test area, since there exists good ground truth for its forests. Further, it is a particularly challenging area because of its hilly topography. Figure 16 is the NED for Kellogg. The elevation in Fig. 16 varies about 50m. The average temperature for the SRTM datatakes for Battle Creek, Michigan, is -2°C [44].

A. Estimation Scenario One: Tree Density and Moisture Assumed Known

In order to test the first estimation scenario, we took tree height and dbh measurements at six of the red pine sites (RP1-6). All of the height measurements were taken using an IMPULSE 200 LR laser rangefinder [45]. We obtained the past basal area per acre for RP1-4 and RP6 and used a stocking chart to convert the dbh and basal area to tree density [46], adjusting the basal area for growth [47]; for RP5 we used dbh and basal area per acre from spreadsheets of thinning studies [42]. The tree density values used, in trees per hectare, are 278(RP1), 250(RP2), 367(RP3), 229(RP4), 586(RP5), and 358(RP6). We set

$M = 0.45\text{g/g}$, the center of our moisture range, and compute estimates of the tree stand height for each stand. Figures 17 and 18 display the raw SRTM-NED heights and the improvement that the estimation algorithm provides using the -2°C thawed and frozen extinction coefficients, respectively, for RP1-6. The “x” marks in Figs. 17 and 18, labeled Raco 1 and Raco 2, are the estimates for two red pine stands at Raco, Michigan, using the 5°C extinction coefficients (not frozen) since the average daylight temperature for those datatakes is roughly 5°C [44]. For these two points, the \bar{h}_{SPC} is obtained by averaging two TOPSAR data takes from two different incidence angles. The $h_{SPC_i}, i = 1, 2$, and the true average heights for the stands are taken from [20]. The tree density values, in trees per hectare, are 1313 (Raco 1) and 876 (Raco 2) [37]. We use $M = 0.45\text{g/g}$. We include the Raco data points to illustrate height retrieval for the 5 to 15m range. Further, the results using the TOPSAR data indicate that the method is independent of the instrument. The TOPSAR points, however, are not included in the accuracy statistics. The mean value of the difference between the estimates and the true average heights for stands RP1-5 assuming thawed conditions is about -1.3m. It is even larger for stands Raco 1 and 2, although these are not included in the statistics. The appreciable non-zero mean value for stands RP1-5 suggests perhaps a bias in the SRTM data or NED, ground and understory return effects (the forward model does not include these), deciduous inclusions (for RP1-5), and/or overestimation of κ_{e_i} . The first could result in a bias up or down. The second and the last certainly would drive the estimate down. The third probably would drive the estimate down, since the deciduous trees were defoliated during the SRTM overpasses, although deciduous inclusions taller than the surrounding red pine might drive the estimate higher. The mean value of the difference between the estimates and the true average heights for stands RP1-5 assuming frozen conditions is about 1.6m, indicating that perhaps the approximate conversion from thawed to frozen extinction coefficients is excessive in this case. Since there is a bias, the spread of the estimates about the actual values is best expressed in root mean square (rms) values. The rms of the difference between the estimates and the true average heights is 3.4m (3.6m for frozen conditions). In order to see how much of an improvement the model introduces to the raw SRTM-NED heights, we note that the mean of the difference between

them and the true average heights is about -7.9m , and the rms of the differences is about 8.3m . Refer to Table V for a listing of the data. The reason why the mean is negative is because SRTM penetrates the canopy to a certain extent. Tree height, density, incidence angle, moisture content, polarization, tree structure, etc. all influence the degree of penetration, hence the need for a model to adjust the observed raw SRTM-NED height up closer to the true h_v .

Another indication of the performance of the algorithm is percent relative error, which is the ratio in percent of the difference between the estimates and the true average heights. In the case of this first estimation scenario used on RP1-6, the mean and rms of the relative errors are -5.4% and 15.1% , respectively. The corresponding values for frozen conditions are 6.0% and 16.8% . For the raw SRTM-NED heights, the mean and rms of the relative errors are -34.0% and 35.5% . See Tables III and IV, line one, for a summary of the above results.

B. Estimation Scenario Two: Tree Density and Moisture are Rough, Approximate Values

Next we process the data for RP1-6 using the second estimation scenario. The results using the -2°C thawed and frozen extinction coefficients, respectively, are depicted in Figs. 19 and 20. The dots are the value of \hat{h}_v for rough values for n and M : $n = 360$ trees/ha (the average density for stands RP1 to RP5) and $M = 0.45$ g/g (the moisture value we used for stands RP1 to RP5 in scenario one). As in the first estimation scenario, the “x” marks are the height estimates of the Raco stands using the n and M values and temperature from scenario one. The upward and downward pointing triangles are the minimum and maximum estimates, illustrating the sensitivity of \hat{h}_n to $\pm 50\%$ errors in n and $\pm 33\%$ errors in M . The open circles are the raw SRTM-NED heights. As before we report the mean and the rms of the difference between the estimates and the actual average heights for thawed and frozen conditions: -1.3m and 3.4m and 1.3m and 3.6m . The corresponding values for the raw SRTM-NED heights are -7.9m and 8.3m , respectively. The mean and rms of the relative errors are -7.2% and 14.3% and 4.6% and 14.8% (thawed and frozen) for the estimation algorithm and -34.0% and 35.5% for the raw SRTM-NED heights. See Tables III and IV, line two. As in scenario one, the estimates are a significant improvement over the

raw SRTM-NED heights.

In order to populate the plots with more stands, we add another red pine stand for which we have only height data, RP7, and use a site index curve [48] to provide true average heights for four other red pine stands RP8-11, similar to the approach used in [21], [22]. A site index curve predicts the height of trees in a stand based on height measurements in the past and the age of the stand. Additionally, two Austrian pine stands (AP1-2) are included, too, using the red pine site index curve. The site index curve is [47]

$$h_v = 1.890S \left(1 - e^{-0.01979A}\right)^{1.3892},$$

where A is the age of the stand in years. S is the site index, base 50, which is the average height of the stand at age 50. Note that since we require h_v in meters, S also is in meters here.

We run the estimation algorithm on all 13 stands. The results are plotted in Fig. 21 and 22 for the -2°C thawed and frozen extinction coefficients, respectively. Again, the Raco stands are assumed at 5°C with n and M values as in scenario one. The mean and the rms of the difference between the estimates and the actual average heights, not including the two Raco points, are -0.6m and 2.5m , respectively (1.6 and 3.0m for frozen conditions). The value for the mean of the raw SRTM-NED heights is -6.1m . The rms of the raw SRTM-NED heights is 6.8m . The mean and rms of the relative errors in the estimates are -1.9% and 21.3% , respectively (14.0% and 26.2% for frozen conditions). For the raw SRTM-NED heights, the mean and rms of the relative errors are -33.1% and 34.4% . See line three of Tables III and IV. Note that the level of accuracy displayed by this algorithm is sufficient at least for separating the three height classes in the Raco red pines used in the allometric equations in Figs. 4 and 5.

VII. CONCLUSIONS AND FUTURE WORK

This paper presented a red pine tree height estimation algorithm that uses Shuttle Radar Topography Mission (SRTM) heights and ancillary data, such as the National Elevation Dataset (NED). The NED was subtracted from the SRTM heights to provide an estimate of the SRTM scattering phase center (SPC)

height, which was then adjusted to yield an estimate of tree height by inverting a forward scattering model. The algorithm produced tree height estimates that were significantly closer to the true tree height than the raw SRTM-NED heights. The algorithm yielded rms errors of 2.5 to 3.6m, compared with the 6.8 to 8.3m rms errors from the raw SRTM-National Elevation Dataset (NED) heights.

Since the SRTM data set is nearly global, and the NED covers all of the United States, the method developed here could be applied to large portions of the United States. Determining which portions would require more data and studies. However, the use of the single-layer model with no ground interaction limits applicability to stands where the ground interaction is small compared to that of the direct backscatter, although the general method could employ a more sophisticated model taking the ground return into account. Additionally, the model currently used could be inaccurate for steep slopes, such as in mountainous areas. Success in tree height retrieval in mountainous areas [16], though, indicates that this limitation could be overcome by including a non-zero slope, as in [2]. Further, the current method is limited to single-species stands, but it could be extended to account for mixed-species stands. More wide-spread use would also involve optimal, region-specific algorithms that could be developed to work in conjunction with the National Land Cover Data (NLCD) 1992 [49], also available from the EROS Data Center. The NLCD could be used to determine whether an area is populated by coniferous or deciduous trees. Then, a region-specific extinction coefficient model, based on the expected composition of typical coniferous and deciduous forests for that area, could be selected to estimate the average tree height.

It is expected that, based on the results in this paper, that any tree density and moisture information will generally improve the height estimates, provided that the forward model relating tree stand height to SRTM SPC height includes all of the dominant scattering mechanisms. As demonstrated in Section VI, such information probably would not even need to be too accurate to have a noticeably positive effect on the height estimates. Methods for estimating tree density directly, or via basal area estimates from which tree density can be derived given allometric equations, are in the SAR literature. Also, recent advances in optical and infrared imaging have made individual tree crown (ITC) forest analysis using satellite

images possible. According to [40], remotely sensed images of 10-100cm resolution show promise for ITC analysis. Estimates of the tree moisture probably would be more difficult to obtain. However, it might be possible to obtain approximate values from extrapolation of ground truth or from other remote sensing techniques, such as in [39]. Global extension of the method in this paper would rely on accurate ground height data, such as the NED, as well as on obtaining valid, approximate values of tree density and moisture. Use of probability distributions for n and M could also be explored.

ACKNOWLEDGMENTS

The authors thank Greg Kowalewski for helping us obtain ground truth data at the W.K. Kellogg Experimental Forest. We also acknowledge Wayne S. Walker for providing in-field training on characterizing tree stands and Josef M. Kellndorfer for suggesting we use Kellogg in this study and for introducing us to Greg Kowalewski. Finally, we thank Matt Gilgenbach for modification of Yi-Cheng Lin's fractal tree modeling routines for the code used in this study.

REFERENCES

- [1] Tom G. Farr *et al.*, "The Shuttle Radar Topography Mission," *Reviews of Geophysics*, vol. 45, 2007.
- [2] Robert N. Treuhaft, Soren N. Madsen, Mahta Moghaddam, and Jakob J. van Zyl, "Vegetation characteristics and underlying topography from interferometric radar," *Radio Science*, vol. 31, no. 6, pp. 1449–1485, November-December 1996.
- [3] Robert N. Treuhaft and Paul R. Siqueira, "Vertical structure of vegetated land surfaces from interferometric and polarimetric radar," *Radio Science*, vol. 35, no. 1, pp. 141–177, January-February 2000.
- [4] Yutaka Kobayashi, Kamal Sarabandi, Leland Pierce, and M. Craig Dobson, "An evaluation of the JPL TOPSAR for extracting tree heights," *IEEE Transactions on Geoscience and Remote Sensing*, vol. 38, no. 6, pp. 2446–2454, November 2000.
- [5] Robert N. Treuhaft, Beverly E. Law, Gregory P. Asner, and Scott Hensley, "Vegetation profile estimates from multialtitude, multifrequency radar interferometric and polarimetric data," in *Proceedings of the the International Geoscience and Remote Sensing Symposium*, 2000.
- [6] Yi-Cheng Lin and Kamal Sarabandi, "Retrieval of forest parameters using a fractal-based coherent scattering model and a genetic algorithm," *IEEE Transactions on Geoscience and Remote Sensing*, vol. 37, no. 3, pp. 1415–1424, May 1999.
- [7] Shane Robert Cloude and Konstantinos Papathanassiou, "Polarimetric SAR interferometry," *IEEE Transactions on Geoscience and Remote Sensing*, vol. 36, no. 5, pp. 1551–1565, September 1998.

- [8] Konstantinos P. Papathanassiou and Shand R. Cloude, "Single-baseline polarimetric sar interferometry," *IEEE Transactions on Geoscience and Remote Sensing*, vol. 39, no. 11, pp. 2352–2363, November 2001.
- [9] Robert N. Treuhaft and Shane R. Cloude, "The structure of oriented vegetation from polarimetric interferometry," *IEEE Transactions on Geoscience and Remote Sensing*, vol. 37, no. 5, pp. 2620–2624, September 1999.
- [10] I.H. Woodhouse, S. Cloude, K. Papathanassiou, J. Hope, J. Suarez, P. Osborne, and G. Wright, "Polarimetric interferometry in the Glen Affric project: Results & conclusions," in *IEEE International Geoscience and Remote Sensing Symposium*, 2002, vol. 2, pp. 820–822.
- [11] S.R. Cloude and K.P. Papathanassiou, "Three-stage inversion process for polarimetric SAR interferometry," *IEE Proceedings-Radar, Sonar and Navigation*, vol. 150, no. 3, pp. 125–134, June 2003.
- [12] Jan Askne, Maurizio Santoro, Gary Smith, and Johan E.S. Fransson, "Multitemporal repeat-pass SAR interferometry of boreal forests," *IEEE Transactions on Geoscience and Remote Sensing*, vol. 41, no. 7, pp. 1540–1550, July 2003.
- [13] Jan Askne and Maurizio Santoro, "Multitemporal repeat pass SAR interferometry of boreal forests," *IEEE Transactions on Geoscience and Remote Sensing*, vol. 43, no. 6, pp. 1219–1228, June 2005.
- [14] C.G. Brown and K. Sarabandi, "Estimation of red pine tree height using Shuttle Radar Topography Mission and ancillary data," in *Proceedings of the International Geoscience and Remote Sensing Symposium*, July 2003, vol. 4, pp. 2850–2852.
- [15] Charles G. Brown, *Tree Height Estimation Using Shuttle Radar Topography Mission and Ancillary Data*, Ph.D. thesis, The University of Michigan, 2003.
- [16] Josef Kellndorfer, Wayne Walker, Leland Pierce, Craig Dobson, Jo Ann Fites, Carolyn Hunsaker, John Vonad, and Michael Clutter, "Vegetation height estimation from Shuttle Radar Topography Mission and National Elevation Datasets," *Remote Sensing of Environment*, vol. 93, no. 3, pp. 339–358, November 2004.
- [17] L. Kenyi, R. Dubayah, M. Hofton, J.B. Blair, and M. Schardt, "Comparison of SRTM-NED data to lidar derived canopy metrics," in *IEEE International Geoscience and Remote Sensing Symposium*, 2007, pp. 2825–2829.
- [18] Yi-Cheng Lin, *A Fractal-Based Coherent Scattering and Propagation Model for Forest Canopies*, Ph.D. thesis, University of Michigan, October 1997.
- [19] Kamal Sarabandi and Adib Nashashibi, "Analysis and applications of backscattered frequency correlation function," *IEEE Transactions on Geoscience and Remote Sensing*, vol. 37, no. 4, pp. 1895–1905, July 1999.
- [20] Yutaka Kobayashi, Kamal Sarabandi, Leland Pierce, and M. Craig Dobson, "An evaluation of the JPL TOPSAR for extracting tree heights," *IEEE Transactions on Geoscience and Remote Sensing*, vol. 38, no. 6, pp. 2446–2454, November 2000.
- [21] P. Saich, H. Balzter, A. Luckman, and L. Skinner, "Deriving forest characteristics using polarimetric InSAR measurements and models," in *Proceedings of the International Geoscience and Remote Sensing Symposium*, 2001, vol. 7, pp. 3096–3098.
- [22] H. Balzter, P. Saich, A.J. Luckman, L. Skinner, and J. Grant, "Forest stand structure from airborne polarimetric INSAR," in *Proceedings of the 3rd International Symposium Retrieval of Bio and Geophysical Parameters from SAR Data for Land Applications*, September 2001, pp. 321–326, ESA SP-475, January 2002.
- [23] United States Geological Survey, "National Elevation Dataset fact sheet 148-99," <http://egsc.usgs.gov/isb/pubs/factsheets/fs14899.html>,

September 1999.

- [24] Dean Gesch, Michael Oimoen, Susan Greenlee, Charles Nelson, Michael Steuck, and Dean Tyler, "The National Elevation Dataset," *Photogrammetric Engineering and Remote Sensing*, vol. 68, no. 1, January 2002.
- [25] Eric Ramirez, "Shuttle Radar Topography Mission: Public distribution," http://www.jpl.nasa.gov/srtm/pub_dist.htm, February 2002.
- [26] EROS Data Center, "National Elevation Dataset (NED)," <http://edc.usgs.gov/products/elevation/ned.html>, August 2002.
- [27] National Imagery and Mapping Agency (NIMA) Geodesy and Geophysics Department, "Department of Defense world geodetic system 1984: Its definition and relationships with local geodetic systems," Tech. Rep. TR8350.2, National Imagery and Mapping Agency, January 2000.
- [28] "NGS geodetic tool kit program descriptions," <http://www.ngs.noaa.gov/TOOLS>, April 2002.
- [29] National Imagery and Mapping Agency (NIMA), "Geographic Translator (GEOTRANS)," <http://164.214.2.59:80/GandG/geotrans/geotrans.html>, May 2002, Version 2.2.1.
- [30] Richard A. Snay, "Using the HTDP software to transform spatial coordinates across time and between reference frames," *Surveying and Land Information Systems*, vol. 59, no. 1, pp. 15–25, 1999.
- [31] C.G. Brown Jr, K. Sarabandi, and L.E. Pierce, "Validation of the Shuttle Radar Topography Mission height data," *IEEE Transactions on Geoscience and Remote Sensing*, vol. 43, no. 8, pp. 1707–1715, August 2005.
- [32] EROS Data Center, "Shuttle Radar Topography Mission (SRTM) finished data, National Elevation Dataset (NED), National Land Cover Data set (NLCD) 2001," <http://seamless.usgs.gov>, March 2008.
- [33] Yi-Cheng Lin and Kamal Sarabandi, "A monte carlo coherent scattering model for forest canopies using fractal-generated trees," *IEEE Transactions on Geoscience and Remote Sensing*, vol. 37, no. 1, pp. 440–451, January 1999.
- [34] Kamal Sarabandi, " Δk -radar equivalent of interferometric SAR's: A theoretical study for determination of vegetation height," *IEEE Transactions on Geoscience and Remote Sensing*, vol. 35, no. 5, pp. 1267–1276, September 1997.
- [35] David Ballester-Berman and Juan M. Lopez-Sanchez, "Coherence loci for a homogeneous volume over a double-bounce ground return," *IEEE Geoscience and Remote Sensing Letters*, vol. 4, no. 2, pp. 317–321, April 2007.
- [36] Jorgen Dall, "InSAR elevation bias caused by penetration into uniform volumes," *IEEE Transactions on Geoscience and Remote Sensing*, vol. 45, no. 7, pp. 2319–2324, July 2007.
- [37] Kathleen M. Bergen, M. Craig Dobson, Terry L. Sharik, and Ian Brodie, "Structure, composition, and above-ground biomass of SIR-C/X-SAR and ERS-1 forest test stands 1991-1994, Raco Michigan site," Tech. Rep. 026511-7-T, Radiation Laboratory, Department of Electrical Engineering and Computer Science, The University of Michigan, Ann Arbor, MI, October 1995.
- [38] Kathleen M. Bergen, M. Craig Dobson, Leland E. Pierce, Josef Kellndorfer, and Paul Siqueira, "October 1994 SIR-C/X-SAR mission: Ancillary data report Raco, Michigan site," Tech. Rep. 026511-6-T, Radiation Laboratory, Department of Electrical Engineering and Computer Science, The University of Michigan, Ann Arbor, MI, October 1995.
- [39] Mahta Moghaddam and Sasan S. Saatchi, "Monitoring tree moisture using an estimation algorithm applied to SAR data from BOREAS," *IEEE Transactions on Geoscience and Remote Sensing*, vol. 37, no. 2, pp. 901–916, March 1999.

- [40] F.A. Gougeon and D. Leckie, "Individual tree crown image analysis: A step towards precision forestry," in *Proceedings of First International Precision Forestry Symposium*, Seattle, Washington, June 2001.
- [41] "Michigan agricultural experiment station: W.K. Kellogg experimental forest," <http://www.maes.msu.edu/ressta/kelloggforest>, December 2001.
- [42] "W.K. Kellogg experimental forest GIS database," From Computer at Michigan Agricultural Experiment Station: W.K. Kellogg Experimental Forest, September 2002, Spreadsheets and ARC GIS layers with ground truth data.
- [43] "KBS GIS aerial photography library," <http://lter.kbs.msu.edu/gis/Aerial%20Photo/AO1.HTML>, 2002.
- [44] "Weather Underground," <http://www.wunderground.com>, Weather History.
- [45] "Impulse series," <http://www.lasertech.com>, Laser Technology, Inc.
- [46] Greg Kowalewski, September 2002, Personal Communication.
- [47] Carol A. Hyldahl and Gerald H. Grossman, "User's guide: RPGrow\$: A red pine growth and analysis spreadsheet for the lake states," General Technical Report NC-156, North Central Forest Experiment Station, Forest Service—U.S. Department of Agriculture, 1992 Folwell Avenue, 1993.
- [48] Thomas Eugene Avery and Harold E. Burkhart, *Forest Measurements*, chapter 14, pp. 278–287, McGraw-Hill, Inc., 1994.
- [49] "National land cover data 1992 (NLCD 92)," <http://edc.usgs.gov/products/landcover/nlcd.html>, August 2002.

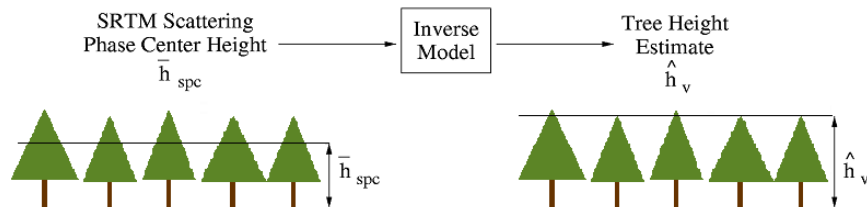


Fig. 1. Ideal inverse model.

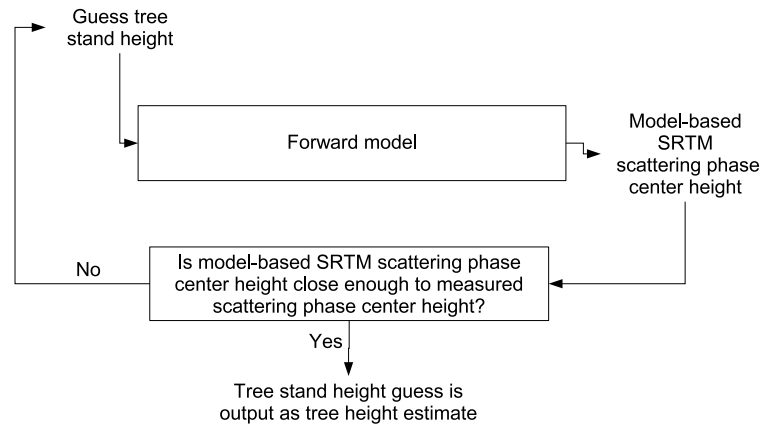


Fig. 2. Block diagram of typical, iterative forward model inversion.

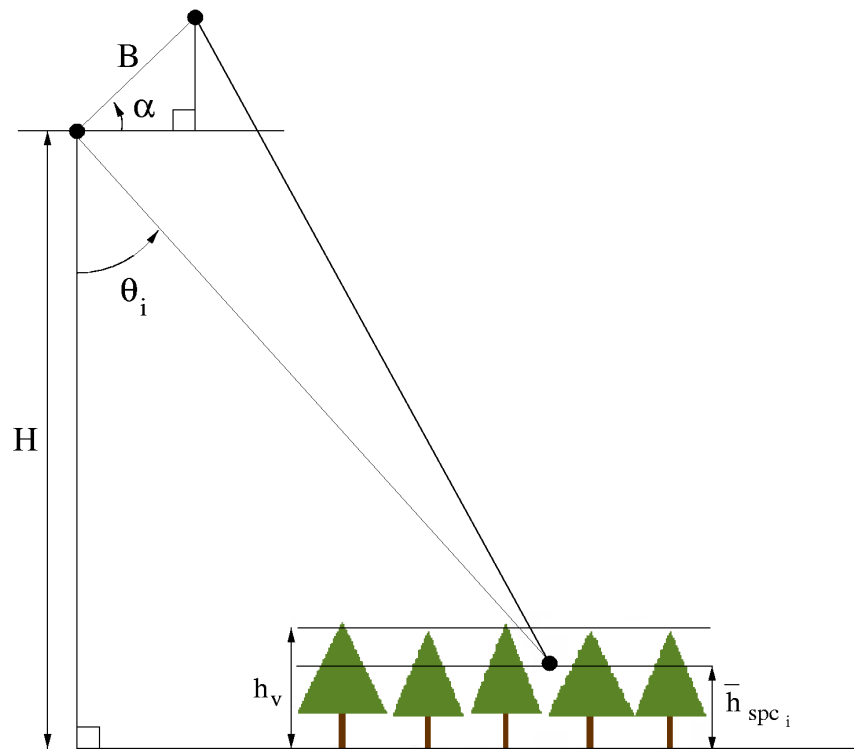


Fig. 3. Interferometric SAR geometry.

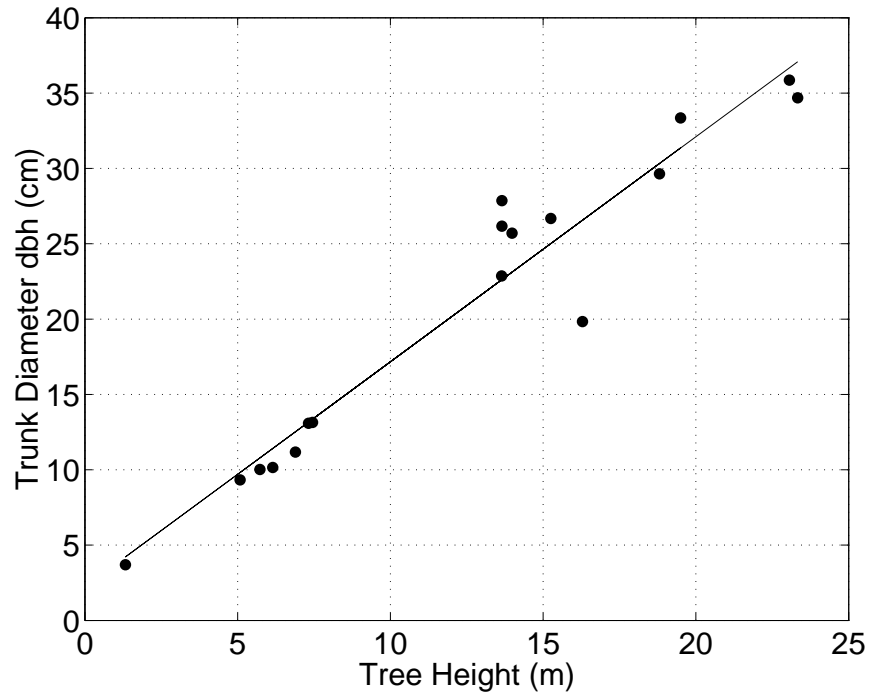


Fig. 4. Allometric equation for diameter at breast height (dbh). Raco, Michigan data from [37] is used to generate the allometric equation.

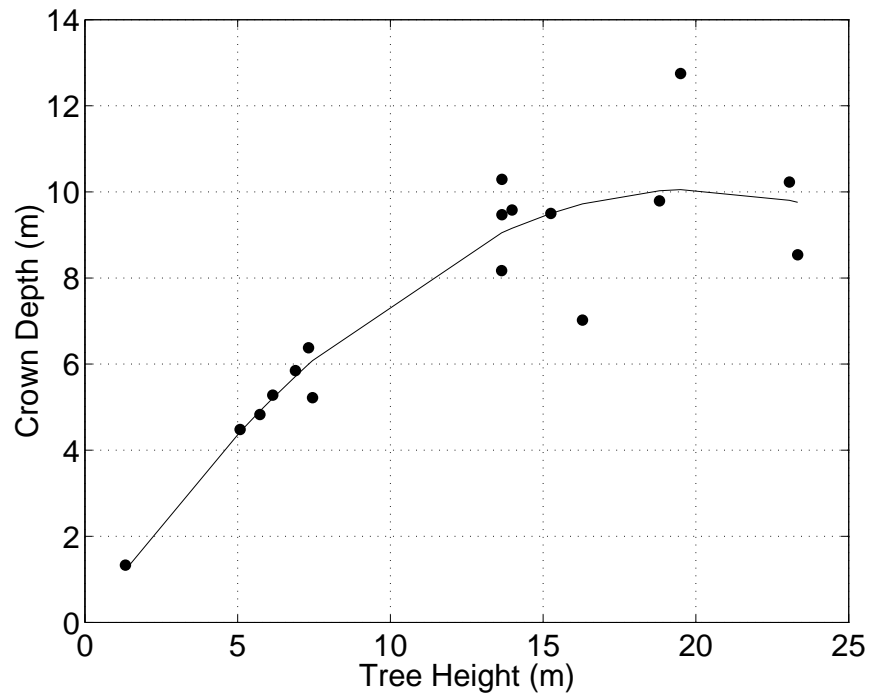


Fig. 5. Allometric equation for crown depth. Raco, Michigan data from [37] is used to generate the allometric equation.

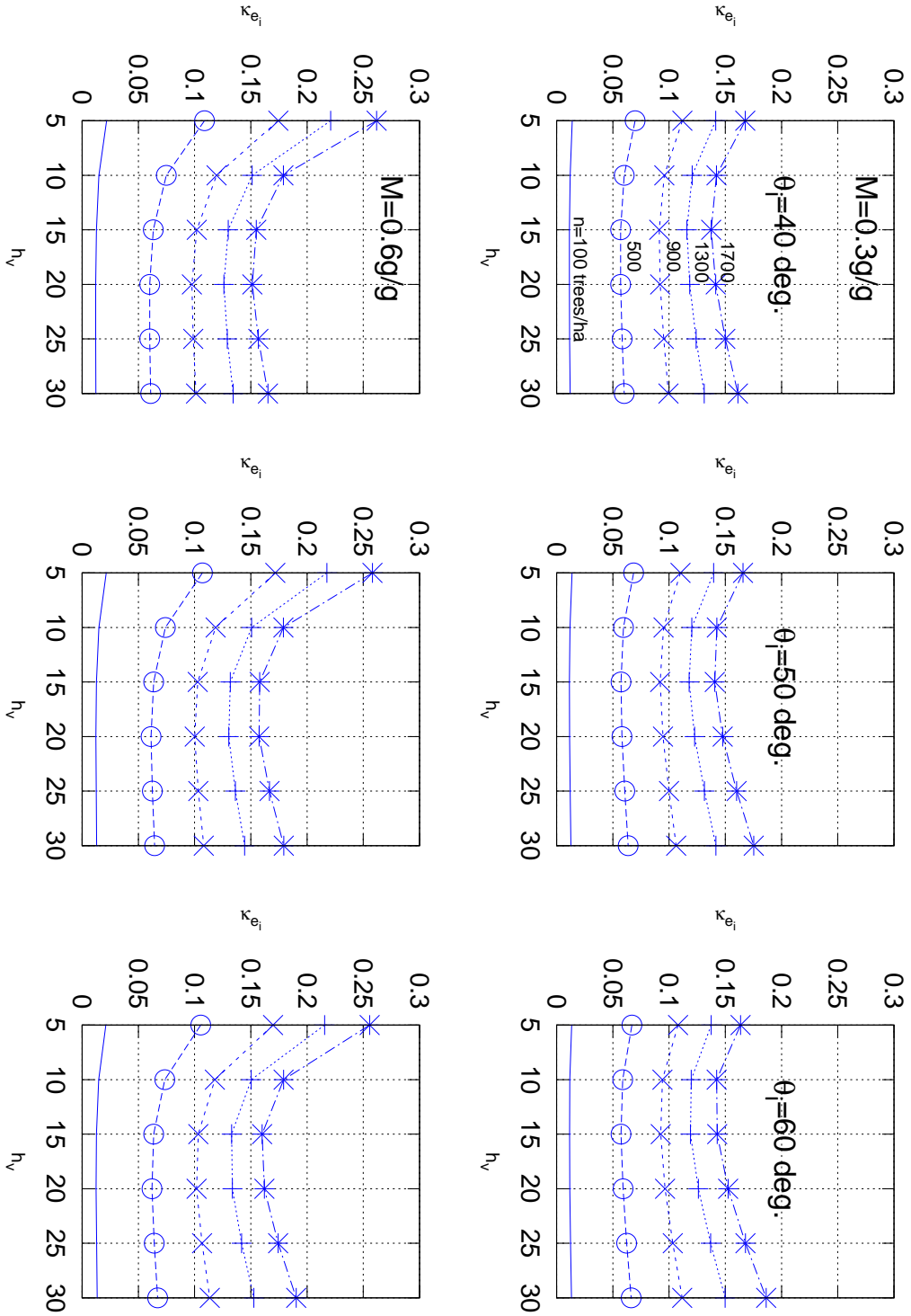


Fig. 6. Plot of VV-polarization extinction coefficient $\kappa_{e_i} = \mathcal{P}_i(h_v, n; \theta_i, M, VV)$ at -2°C . The top row corresponds to low moisture ($M = 0.3 \text{ g/g}$ wet biomass), while in the bottom row the moisture level is higher ($M = 0.6 \text{ g/g}$ wet biomass). The columns, left to right, correspond to incidence angles $\theta_i = 40^\circ, 50^\circ, 60^\circ$. Tree stand height h_v in meters is along the x-axis of the individual subplots. Tree density n is varied within each subplot to produce the lines marked by the different symbols, where the symbols “.”, “o”, “x”, “+”, and “*” correspond to tree densities of $n = 100, 500, 900, 1300, 1700$ trees per hectare.

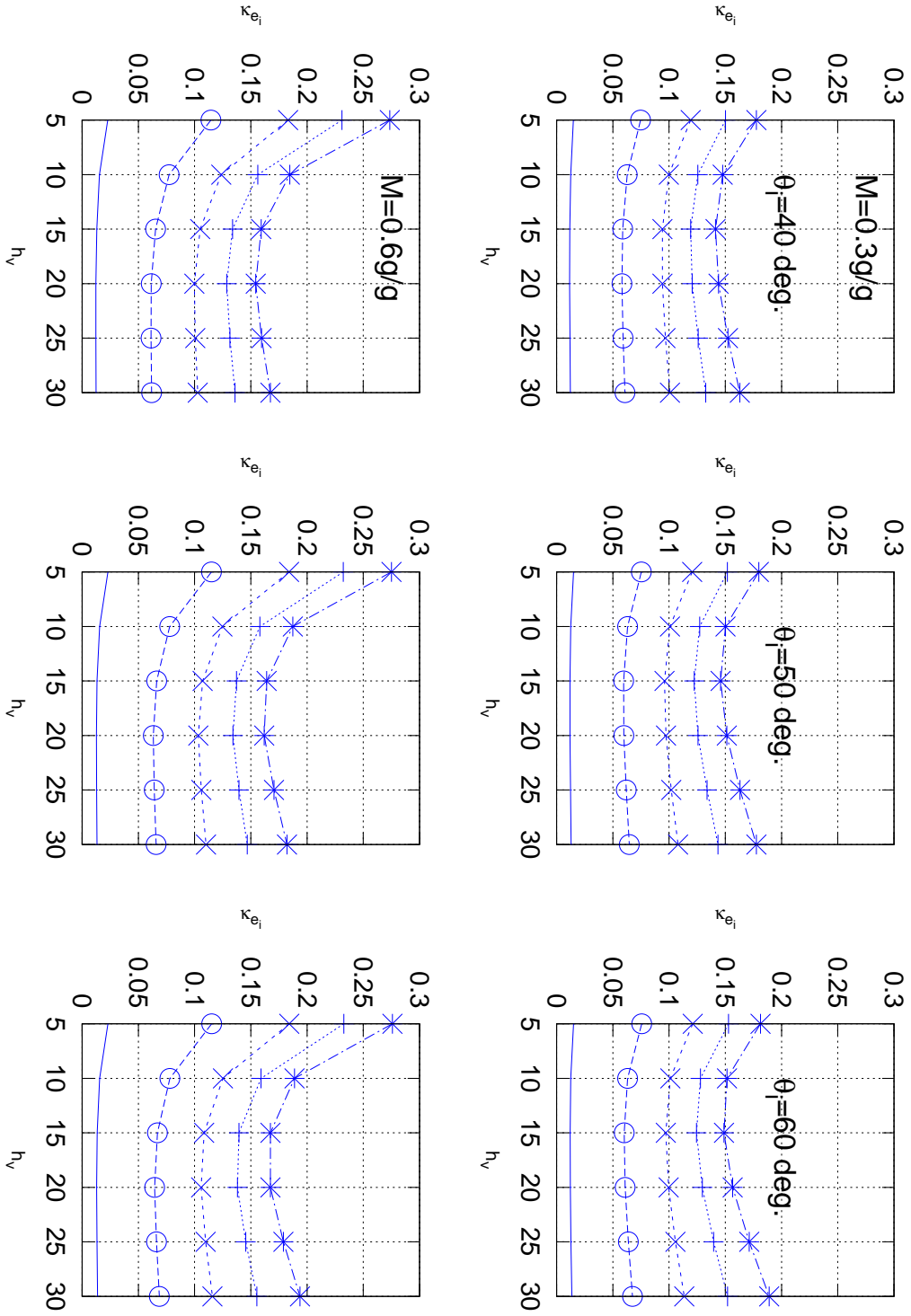


Fig. 7. Plot of HH-polarization extinction coefficient $\kappa_{e_i} = \mathcal{P}_i(h_v, n; \theta_i, M, HH)$ at -2°C . See Fig. 6 for a description of the plot.

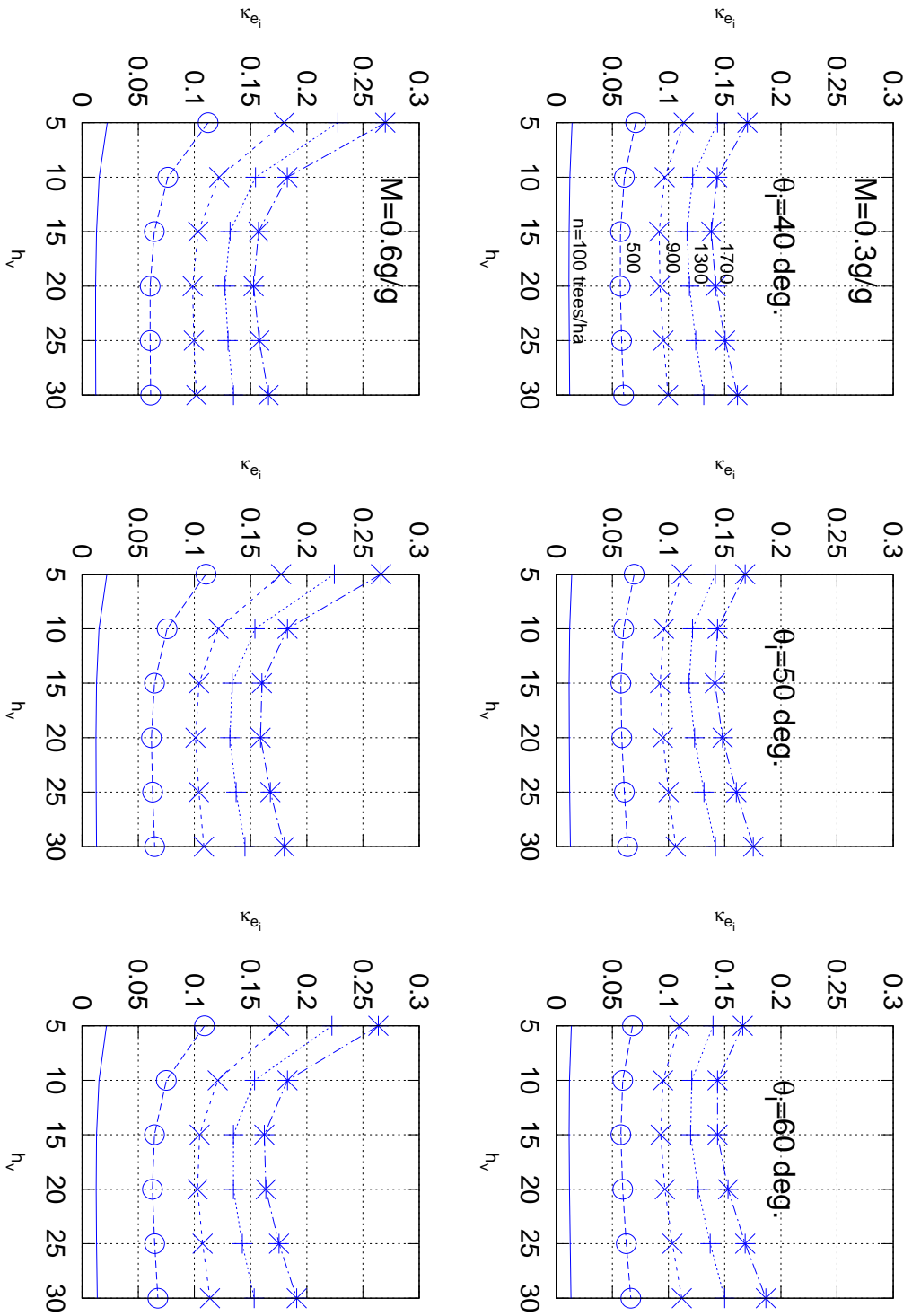


Fig. 8. Plot of VV-polarization extinction coefficient $\kappa_{e_i} = \mathcal{P}_i(h_v, n; \theta_i, M, VV)$ at 5°C . See Fig. 6 for a description of the plot.

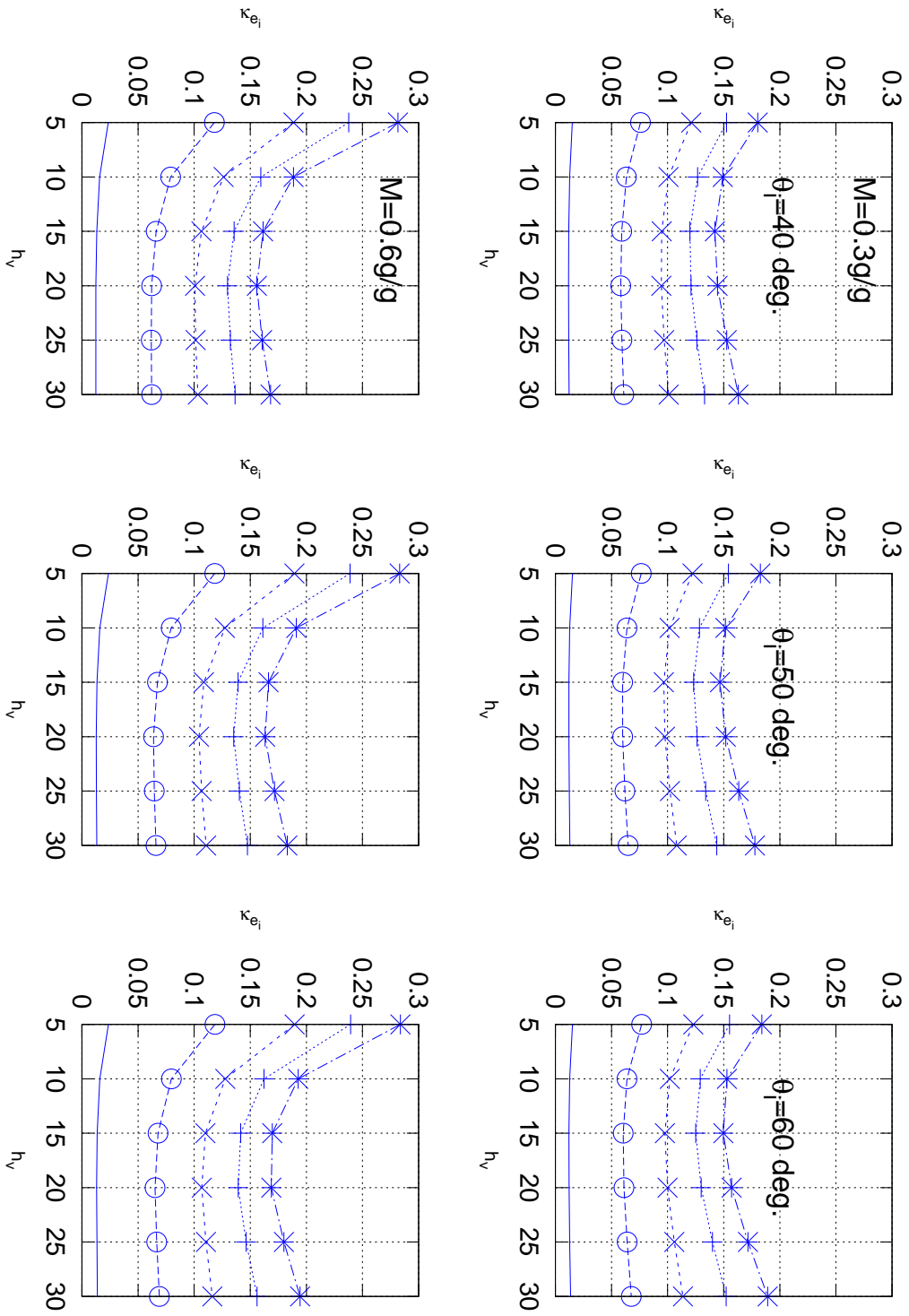


Fig. 9. Plot of HH-polarization extinction coefficient $\kappa_{e_i} = \mathcal{P}_i(h_v, n; \theta_i, M, HH)$ at 5°C . See Fig. 6 for a description of the plot.

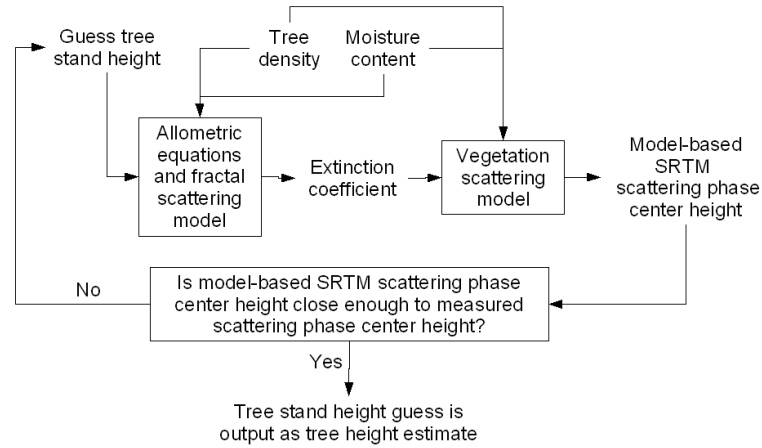


Fig. 10. Block diagram of forward model inversion.

Tree Stand Height Contours (m): Stand RP2, SRTM SPC height = 16.6 m

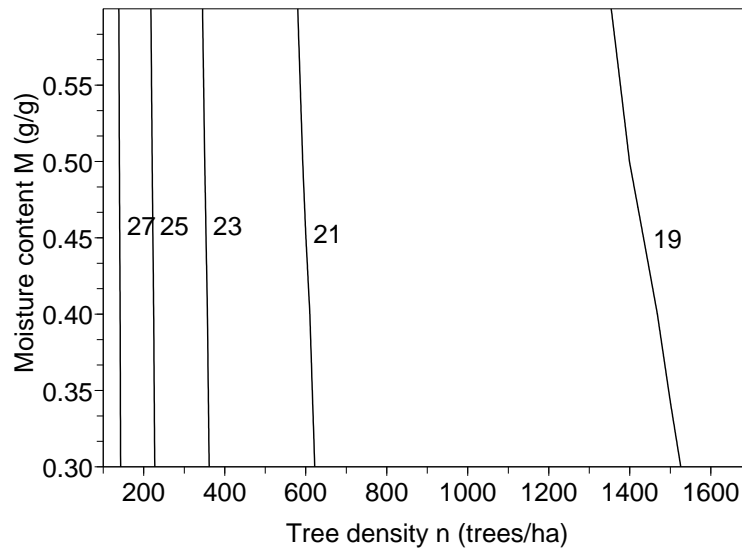


Fig. 11. Contour plot of h_v estimates, in meters, for stand RP2 versus tree density n and moisture content M for -2°C thawed conditions. The plot for 5°C would be essentially the same. First, h_v is estimated for all possible combinations of n and M on a sparse grid. The \hat{h}_v values then are linearly interpolated to a much higher density, with $n = 100, 101, 102, \dots, 1700$ trees/ha and $M = 0.3, 0.31, 0.32, \dots, 0.6$ g/g.

Tree Stand Height Contours (m): Stand AP2, SRTM SPC height = 2.8 m

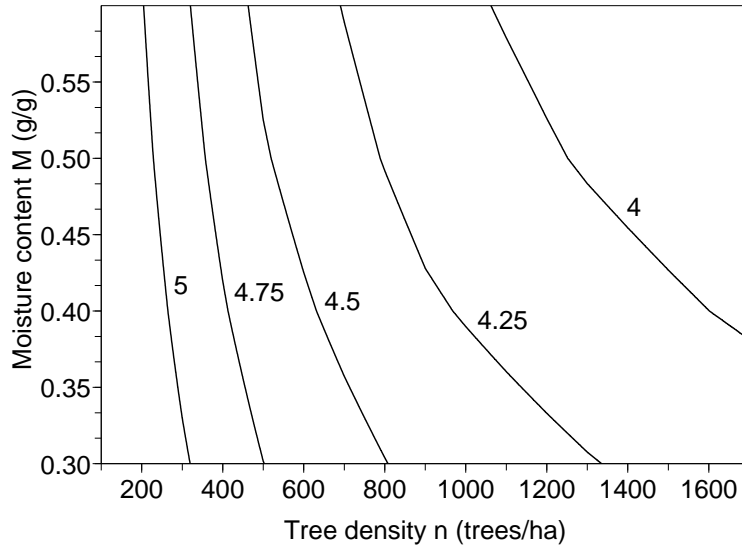


Fig. 12. Contour plot of h_v estimates, in meters, for stand AP2 versus tree density n and moisture content M . See Fig. 11 for a description of this plot.

Tree Stand Height Contours (m): Stand RP8, SRTM SPC height = 8.9 m

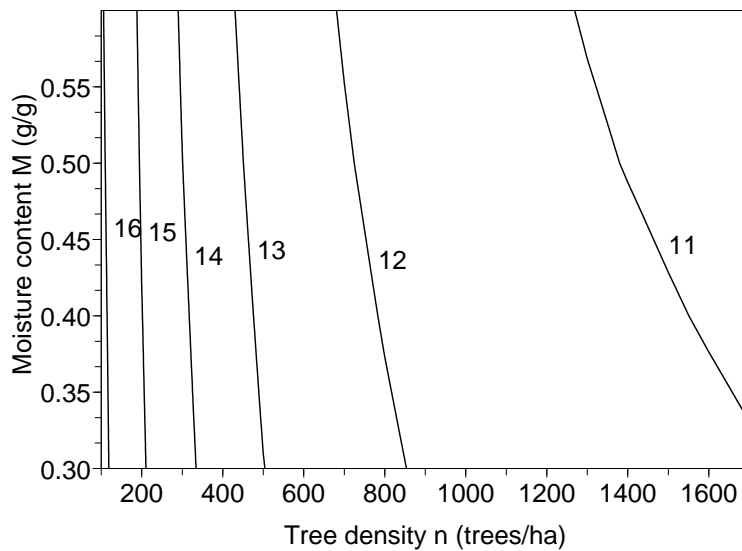


Fig. 13. Contour plot of h_v estimates, in meters, for stand RP8 versus tree density n and moisture content M . See Fig. 11 for a description of this plot.

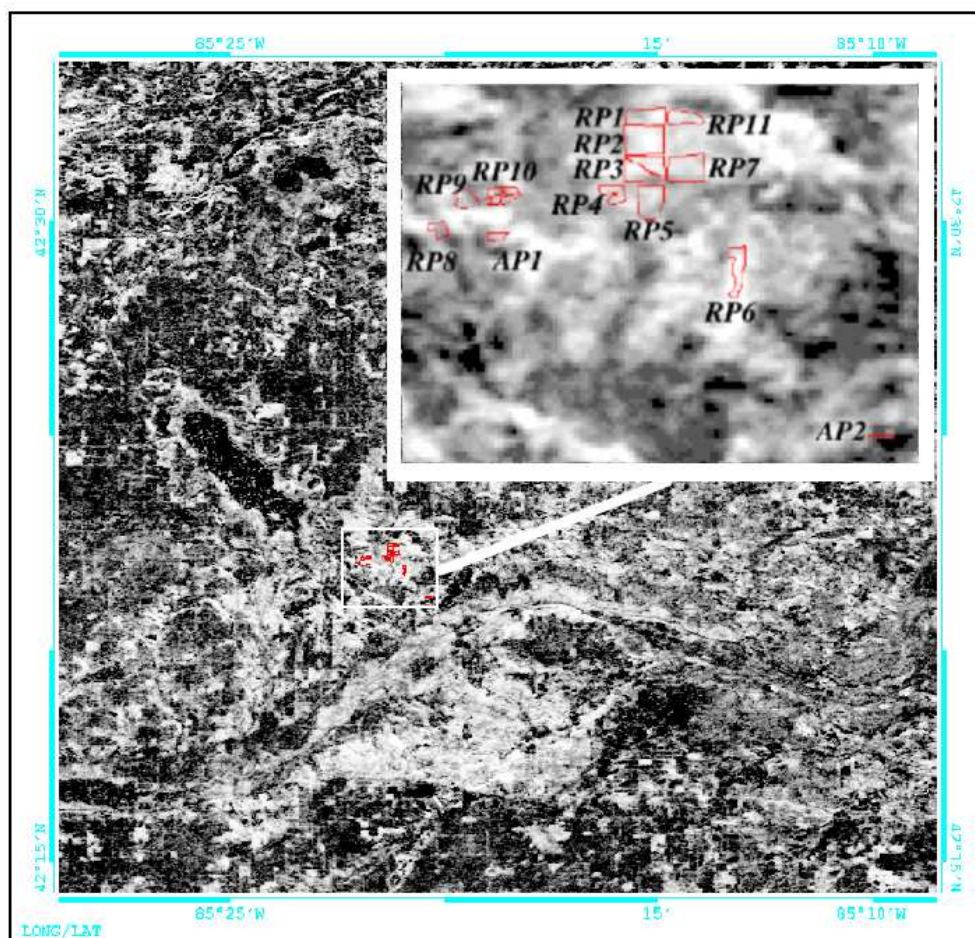


Fig. 14. SRTM minus National Elevation Dataset (NED) heights with overlay of map of W.K. Kellogg Experimental Forest tree stands used in this paper. Darker areas are small height differences, and brighter areas are larger height differences. The red pine stands are labeled “RP”, while the Austrian pine stands are labeled “AP”. Stand areas range from approximately 3 to 45 30m by 30m SRTM pixels.



Fig. 15. Infrared image from 1996 of the same area in Fig. 14 with white overlay of map of W.K. Kellogg Experimental Forest tree stands used in this paper. Darker areas generally correspond to coniferous forests; medium values generally are deciduous forests; and brighter areas usually are bare surface areas.

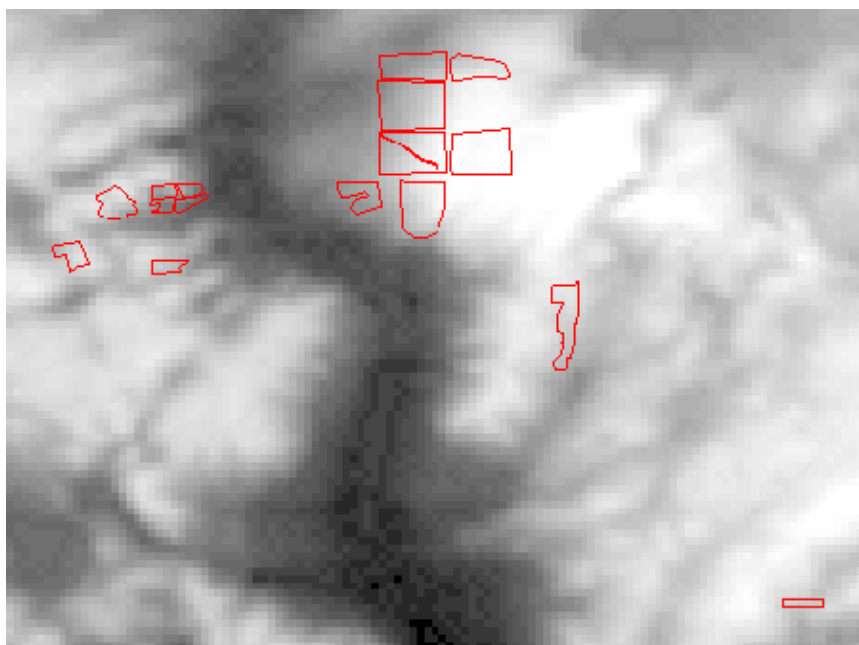


Fig. 16. NED heights with overlay of map of W.K. Kellogg Experimental Forest tree stands used in this paper. See Fig. 14. Darker areas are lower elevations, and brighter areas are higher elevations.

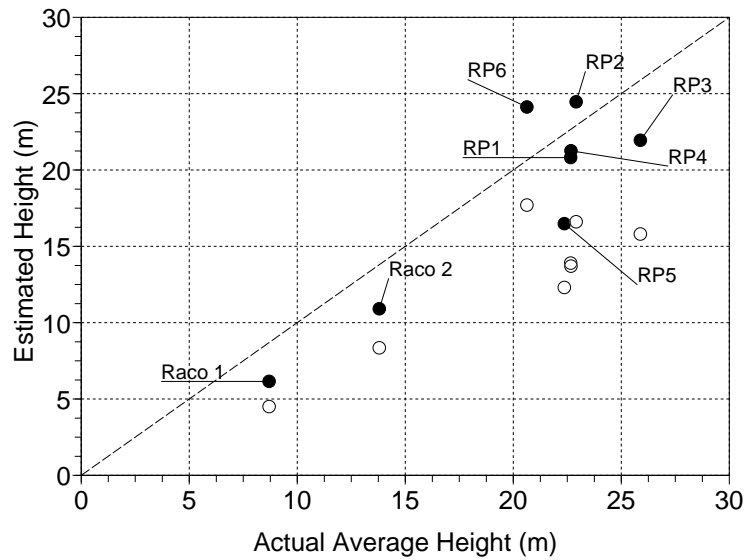


Fig. 17. Results of the first estimation scenario: RP1-6 assuming the densities and moisture values are known and assuming thawed conditions. The open circles are the raw SRTM minus NED heights. See also Tables III and IV, line one. The “x” marks are the estimates for two red pine stands at Raco, Michigan. For these two points, the \bar{h}_{SPC} is obtained by averaging two TOPSAR data takes from two different incidence angles. The Raco stands are not included in the accuracy statistics. Stands RP1-6 use the -2°C extinction coefficients, and the Raco stands use the 5°C extinction coefficients.

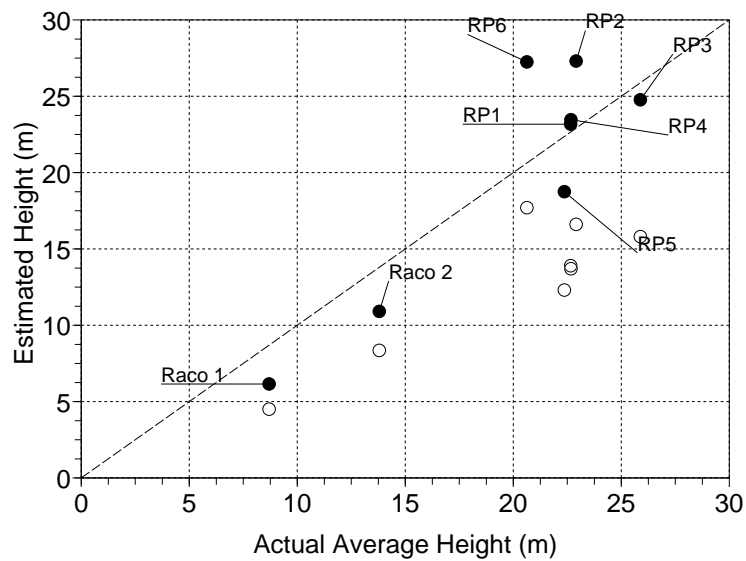


Fig. 18. Results of the first estimation scenario: RP1-6 assuming the densities and moisture values are known and assuming frozen conditions. The open circles are the raw SRTM minus NED heights. See also Tables III and IV, line one. The “x” marks are the estimates for two red pine stands at Raco, Michigan. For these two points, the \bar{h}_{SPC} is obtained by averaging two TOPSAR data takes from two different incidence angles. The Raco stands are not included in the accuracy statistics. Stands RP1-6 use the -2°C extinction coefficients, and the Raco stands use the 5°C extinction coefficients (not frozen).

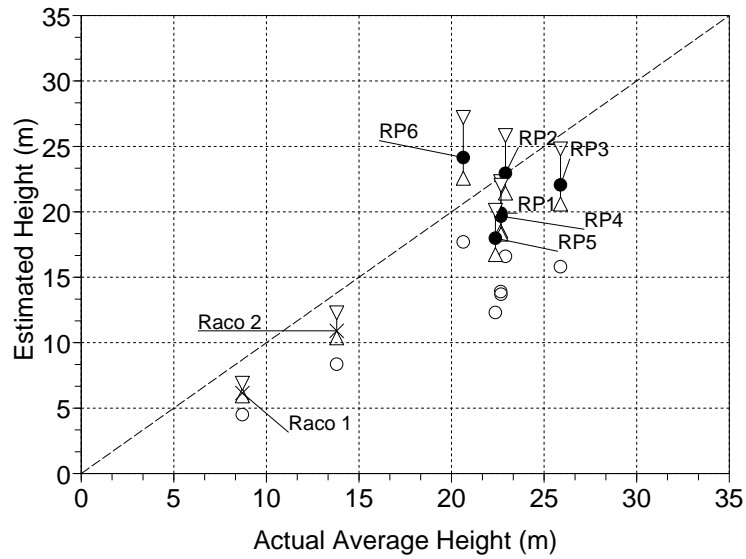


Fig. 19. Results of the second estimation scenario for thawed conditions: RP1-6 assuming density and moisture are rough, approximate values. See also Tables III and IV, line two. The dots are the values of \hat{h}_v for $n = 360$ trees/ha and $M = 0.45$ g/g. The upward and downward pointing triangles are the minimum and maximum estimates, assuming $\pm 50\%$ error in n and $\pm 33\%$ error in M . The open circles are the raw SRTM minus NED heights. Stands RP1-6 use the -2°C extinction coefficients, and the Raco stands use the 5°C extinction coefficients.

Tree Height (rows in meters) / Tree Density (columns in trees/ha)	100	500	900	1300	1700
5	5,100	5,500	5,900	5,1300	5,1700
10	10,100	10,500	10,900	10,1300	10,1700
15	15,100	15,500	15,900	15,1300	15,1700
20	20,100	20,500	20,900	20,1300	20,1700
25	25,100	25,500	25,900	25,1300	25,1700
30	30,100	30,500	30,900	30,1300	30,1700

TABLE I
COMBINATIONS OF TREE HEIGHT AND DENSITY VALUES USED TO GENERATE THE EXTINCTION COEFFICIENT MODEL.

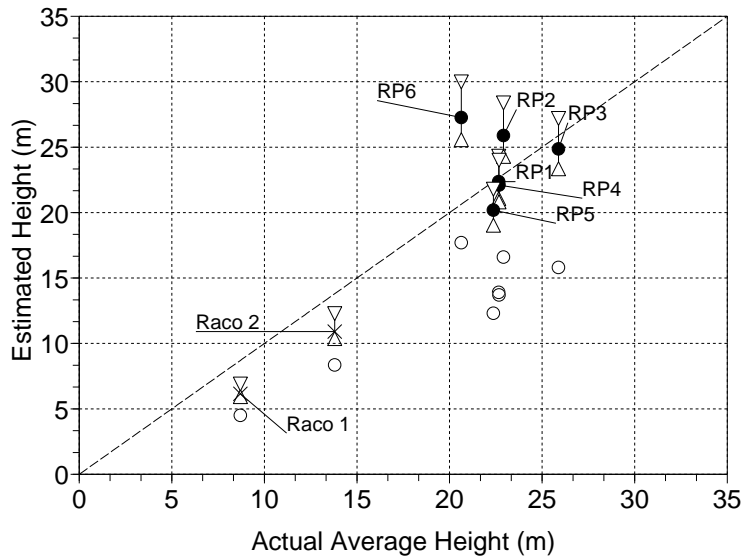


Fig. 20. Results of the second estimation scenario for frozen conditions: RP1-6 assuming density and moisture are rough, approximate values. See also Tables III and IV, line two. The dots are the values of \hat{h}_v for $n = 360$ trees/ha and $M = 0.45$ g/g. The upward and downward pointing triangles are the minimum and maximum estimates, assuming $\pm 50\%$ error in n and $\pm 33\%$ error in M . The open circles are the raw SRTM minus NED heights. Stands RP1-6 use the -2°C extinction coefficients, and the Raco stands use the 5°C extinction coefficients (not frozen).

Incidence Angle (rows in degrees) / Moisture Content (columns in g/g)	0.3	0.4	0.5	0.6
40	40,0.3	40,0.4	40,0.5	40,0.6
45	45,0.3	45,0.4	45,0.5	45,0.6
50	50,0.3	50,0.4	50,0.5	50,0.6
55	55,0.3	55,0.4	55,0.5	55,0.6
60	60,0.3	60,0.4	60,0.5	60,0.6

TABLE II

COMBINATIONS OF INCIDENCE ANGLE AND MOISTURE CONTENT VALUES USED TO GENERATE THE EXTINCTION COEFFICIENT MODEL.

Estimation Scenario	Tree Stands	Raw SRTM-NED		Estimation Algorithm	
		mean difference(m)	rms difference(m)	mean difference(m)	rms difference(m)
Densities and moisture values assumed known	RP1-6	-7.9	8.3	-1.3 (1.3)	3.4 (3.6)
Approximate density and moisture values used	RP1-6	-7.9	8.3	-1.8 (0.9)	3.2 (3.1)
Approximate density and moisture values used	RP1-11, AP1-2	-6.1	6.8	-0.6 (1.6)	2.5 (3.0)

TABLE III

SUMMARY OF TEST RESULTS. THE RAW SRTM-NED MEAN AND RMS DIFFERENCE REFER TO THE MEAN AND ROOT MEAN SQUARE OF THE DIFFERENCE BETWEEN THE RAW SRTM-NED HEIGHTS AND THE TRUE AVERAGE TREE HEIGHTS. THE ESTIMATION ALGORITHM MEAN AND RMS DIFFERENCE ARE THE SAME STATISTICS FOR THE DIFFERENCE BETWEEN THE OUTPUT OF THE ESTIMATION ALGORITHM AND THE TRUE AVERAGE TREE HEIGHTS. THE RESULTS FOR THE FROZEN CONDITIONS ARE IN PARENTHESES.

Estimation Scenario	Tree Stands	Raw SRTM-NED		Estimation Algorithm	
		mean relative error(%)	rms relative error(%)	mean relative error(%)	rms relative error(%)
Densities and moisture values assumed known	RP1-6	-34.0	35.5	-5.4 (6.0)	15.1 (16.8)
Approximate density and moisture values used	RP1-6	-34.0	35.5	-7.2 (4.6)	14.3 (14.8)
Approximate density and moisture values used	RP1-11, AP1-2	-33.1	34.4	1.9 (14.0)	21.3 (26.2)

TABLE IV

SUMMARY OF TEST RESULTS. THE RAW SRTM-NED MEAN AND RMS RELATIVE ERRORS REFER TO THE MEAN AND ROOT MEAN SQUARE OF THE DIFFERENCE BETWEEN THE RAW SRTM-NED HEIGHTS AND THE TRUE AVERAGE TREE HEIGHTS, DIVIDED BY THE TRUE AVERAGE TREE HEIGHTS. THE ESTIMATION ALGORITHM MEAN AND RMS RELATIVE ERRORS ARE THE SAME STATISTICS FOR THE DIFFERENCE BETWEEN THE OUTPUT OF THE ESTIMATION ALGORITHM COMPARED WITH THE TRUE AVERAGE TREE HEIGHTS. THE RESULTS FOR THE FROZEN CONDITIONS ARE IN PARENTHESES.

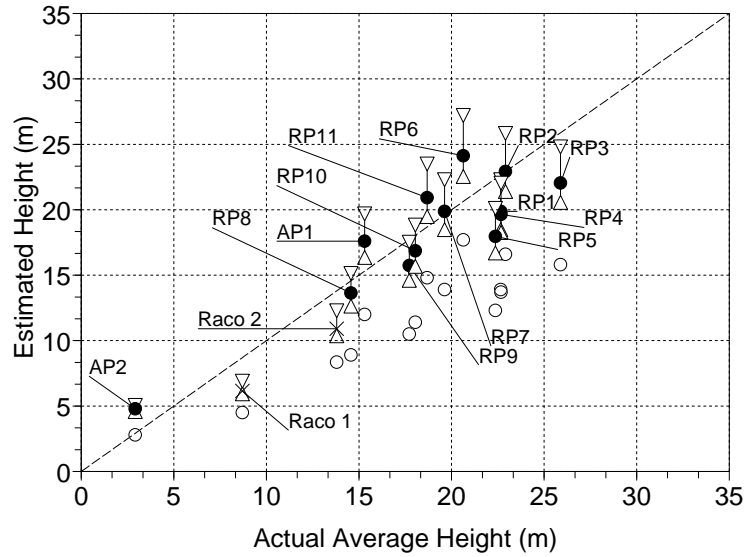


Fig. 21. Results of the second estimation scenario for thawed conditions: RP1-11 and AP1-2 assuming the distributions of the density and moisture values are known. See also Tables III and IV, line three. The dots are the expected values of \hat{h}_v with $n = 360$ trees/ha and $M = 0.45$ g/g. The upward and downward pointing triangles are the minimum and maximum estimates, assuming $\pm 50\%$ error in n and $\pm 33\%$ error in M . The open circles are the raw SRTM minus NED heights. Stands RP1-11 and AP1-2 use the -2°C extinction coefficients, and the Raco stands use the 5°C extinction coefficients.

Tree Stand	Raw SRTM-NED (m)	Actual Average Height (m)	Difference (m)
RP1	13.9	22.7	-8.8
RP2	16.6	22.9	-6.3
RP3	15.8	25.9	-10.1
RP4	13.7	22.7	-9.0
RP5	12.3	22.4	-10.1
RP6	17.7	20.6	-2.9

TABLE V

SUMMARY OF RAW SRTM-NED HEIGHTS, ACTUAL AVERAGE HEIGHTS, AND THE DIFFERENCE BETWEEN THE RAW SRTM-NED AND ACTUAL AVERAGE HEIGHTS FOR RP1-6. THE NEGATIVE DIFFERENCES INDICATE THAT THE RAW SRTM-NED HEIGHTS ARE ON AVERAGE BELOW THE TRUE AVERAGE TREE HEIGHT.

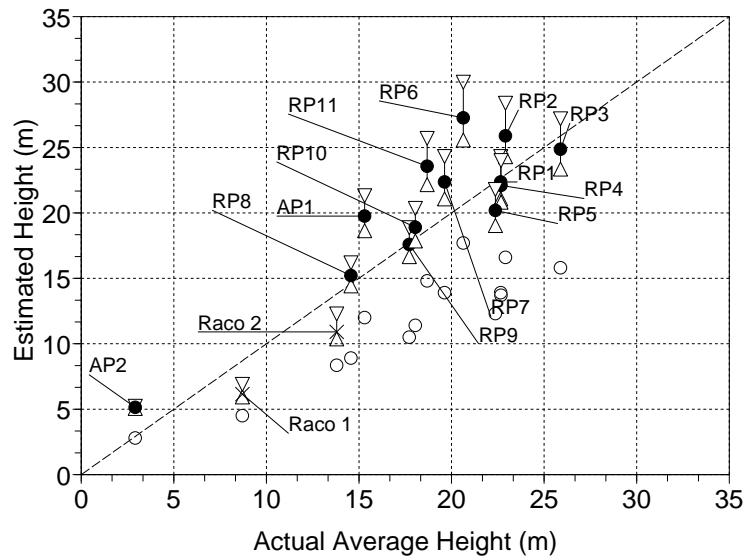


Fig. 22. Results of the second estimation scenario for frozen conditions: RP1-11 and AP1-2 assuming the distributions of the density and moisture values are known. See also Tables III and IV, line three. The dots are the expected values of \hat{h}_v with $n = 360$ trees/ha and $M = 0.45$ g/g. The upward and downward pointing triangles are the minimum and maximum estimates, assuming $\pm 50\%$ error in n and $\pm 33\%$ error in M . The open circles are the raw SRTM minus NED heights. Stands RP1-11 and AP1-2 use the -2°C extinction coefficients, and the Raco stands use the 5°C extinction coefficients (not frozen).

Charles G. Brown Jr. (S'93–M'02) received the B.S. and M.S. degrees in electrical engineering from Brigham Young University, Provo, UT, in 1998 and the Ph.D. degree in electrical engineering and atmospheric, oceanic, and space sciences from The University of Michigan, Ann Arbor, in 2003.

He has a broad spectrum of research experience in electromagnetics (EM) and signal processing. He has worked at Lawrence Livermore National Laboratory, Livermore, CA, since 2003, where his work includes EM analysis and measurement signal processing for lightning safety studies; EM simulation for design and optimization of particle accelerators; and EM modeling and signal processing for EM diagnostics in the National Ignition Facility. His undergraduate and Master's research experience is in algorithm development for remote sensing of near-surface ocean wind using satellite scatterometer data. His Ph.D. research work is in synthetic aperture radar (SAR) and interferometric SAR (INSAR) image modeling and processing for estimation of tree height.

Kamal Sarabandi (S'87–M'90–SM'92–F'00) received the B.S. degree in EE from Sharif University of Technology in 1980. He received the M.S. degree in EE (1986) and the M.S. degree in Mathematics and the Ph.D. degree in electrical engineering from The University of Michigan, Ann Arbor, in 1989. He is the Rufus S. Teesdale professor of Engineering and Director of the Radiation Laboratory in the Department of Electrical Engineering and Computer Science at the University of Michigan. His research areas of interest include microwave and millimeter-wave radar remote sensing, Meta-materials, electromagnetic wave propagation, and antenna miniaturization.

He has 22 years of experience with wave propagation in random media, communication channel modeling, microwave sensors, and radar systems and is leading a large research group including two research scientists, 12 Ph.D. and 2 M.S. students. He has graduated 31 Ph.D. and supervised numerous postdoctoral students. He has served as the Principal Investigator on many projects sponsored by NASA, JPL, ARO, ONR, ARL, NSF, DARPA and a larger number of industries. Currently he is leading the Center for Microelectronics and Sensors funded by the Army Research Laboratory under the Micro-Autonomous Systems and Technology (MAST) Collaborative Technology Alliance (CTA) program.

Dr. Sarabandi has published many book chapters and more than 170 papers in refereed journals on miniaturized and on-chip antennas, meta-materials, electromagnetic scattering, wireless channel modeling, random media modeling, microwave measurement techniques, radar calibration, inverse scattering problems, and microwave sensors. He has also had more than 420 papers and invited presentations in many national and international conferences and symposia on similar subjects.

Dr. Sarabandi is a member of NASA Advisory Council appointed by the NASA Administrator. He also served as a vice president of the IEEE Geoscience and Remote Sensing Society (GRSS) and a member of the IEEE Technical Activities Board Awards Committee. He is serving on the Editorial Board of The IEEE Proceedings, and served as Associate Editor of the IEEE Transactions on Antennas and Propagation and the IEEE Sensors Journal. Professor Sarabandi is a member of Commissions F and D of URSI and is listed in American Men & Women of Science Who's Who in America and Who's Who in Science and Engineering. Dr. Sarabandi was the recipient of the Henry Russel Award from the Regent of The University of Michigan. In 1999 he received a GAAC Distinguished Lecturer Award from the German Federal Ministry for Education, Science, and Technology. He was also a recipient of the 1996 EECS Department Teaching Excellence Award and a 2004 College of Engineering Research Excellence Award. In 2005 he received the IEEE GRSS Distinguished Achievement Award and the University of Michigan Faculty Recognition Award. He also received the best paper Award at the 2006 Army Science Conference. In 2008 he was awarded a Humboldt Research Award from The Alexander von Humboldt Foundation of Germany. In the past several years, joint papers presented by his students at a number of international symposia (IEEE APS'95,'97,'00,'01,'03,'05,'06,'07; IEEE IGARSS'99,'02,'07; IEEE IMS'01, USNC URSI'04,'05,'06, AMTA '06, URSI GA 2008) have received student paper awards.

Leland E. Pierce (S'85–M'89–SM'01) received the B.S. degrees in both Electrical and Aerospace Engineering in 1983, and the M.S. and Ph.D. degrees in Electrical Engineering in 1986 and 1991, respectively, all from the University of Michigan, Ann Arbor.

Since then he has been the head of the Microwave Image Processing Facility within the Radiation Laboratory in the Electrical Engineering and Computer Science Department at the University of Michigan, Ann Arbor, where he is responsible for research into the uses of polarimetric SAR systems for remote sensing applications, especially forest canopy parameter inversion.